CHEMPHYSCHEM

Supporting Information

Electrochemically Controlled Proton-Transfer-Catalyzed Reactions at Liquid–Liquid Interfaces: Nucleophilic Substitution on Ferrocene Methanol

Pekka Peljo,[a] Liang Qiao,[b] Lasse Murtomäki,*[a] Christoffer Johans,[a] Hubert H. Girault,[b] and Kyösti Kontturi[a]

cphc_201200953_sm_miscellaneous_information.pdf

Supporting information

Electrochemically Controlled Proton Transfer Catalyzed Reactions at Liquid-Liquid Interfaces: Nucleophilic Substitution on Ferrocene Methanol

Pekka Peljo[a], Liang Qiao[b], Lasse Murtomäki[a,*], Christoffer Johans[a], Hubert H. Girault[b] and Kyösti Kontturi[a]

[a] Department of Chemistry, Aalto University, P.O. Box 16100, 00076 Aalto, Finland

[b] Laboratoire d'Electrochimie Physique et Analytique, Ecole Polytechnique Fédérale de Lausanne (EPFL), Station 6, CH-1015 Lausanne, Switzerland

*Corresponding author

Tel. +358 9 470 22575

Fax +358 9 470 22580

Email lasse.murtomaki@aalto.fi

Contents

1 Materials

All chemicals were used as received. The aqueous solutions were prepared with ultrapure water (Millipore Milli-Q, specific resistivity 18.2 MΩcm). The solvents were 1,2-dichlorobenzene (DCB, ≥ 98%, Fluka), HCl (FF Chemicals, 1 M), ethanol (94%, Altia), and acetone (99.5%, Lab Scan). Ferrocene methanol (FcMeOH, 97%, Aldrich) and Decamethyl ferrocene (DcMFc, 99%, Alfa Aesar) were used as redox mediators. Other chemicals include sodium iodide (99%, Acros), potassium bis(oxalato)oxotitanate(IV) dihydrate (TiOx, Alfa Aesar), tetraethylammonium chloride (TEACl, 98 %, Sigma), agarose (pure, Aldrich Chemie) and indole (99+%, Acros). Equimolar amounts of lithium tetrakis(pentafluorophenyl)borate (LiTB) n-etherate (Boulder Scientific Company) and bis(triphenylphosphoranylidene) ammonium chloride (BACl, 97%, Aldrich) were used to prepare bis(triphenylphosphoranylidene) ammonium tetrakis (pentafluorophenyl) borate (BATB) by metathesis from methanol-water (v/v 2:1) solutions of the respective salts. The resulting precipitate was filtered, washed, and recrystallized from acetone:ethanol (1:1) mixture.[1]

2 Experimental Section

The oil-water interface was polarized chemically by controlling the ionic composition of the respective phases in shake-flask experiments. Equal amounts of a DCB solution containing 5 mM FcMeOH and an acidic aqueous solution (10 mM HCl) containing 5 mM LiTB were added into a vial establishing a Galvani potential difference of 0.67 V across the interface (For the calculation of the potential difference and the distribution of species, see Section 6). The two phases were vigorously mixed with a magnetic stirrer for various reaction times and left to settle for 30 s. After phase separation, the aqueous phase was analyzed for hydrogen peroxide using NaI and titanium oxalate methods.[2] A dedicated three-channel microchip (Figure 1) was used as an emitter in ESI-MS to analyze the products of the two-phase reactions. Samples taken from the DCB phase or the fresh solution were infused via channel A at the flow rate of 6 μl/h, while channel B was blocked. A sheath flow of ESI buffer (50% water, 49% methanol and 1% acetic acid) was infused via channel C at the flow rate of 54 μl/h to stabilize ESI performance. High voltage (+3.7 kV) was applied to the electrode to induce ESI. A linear ion trap mass spectrometer (Thermo LTQ Velos) was used to characterize the emitted ions. For online analysis of the reaction products, the aqueous and oil phases were infused into different channels of the microchip (A and B) at equal flow rates with a

syringe pump and the ESI buffer was infused into channel C. The total flow rate of the outlet was kept constant at 60 μl/h, while the flow rates in channels A and B were varied for various reaction times (from 30 s to 3 min).

3 Electrochemical measurements

3.1 Ion transfer voltammetry

All electrochemical measurements at a liquid-liquid interface were performed at ambient temperature (22 ± 1 °C) under aerobic conditions in a Faraday cage. *iR* compensated cyclic voltammograms (CVs) at the water-DCB interface were recorded with an Autolab four-electrode potentiostat PGSTAT100 (EcoChemie, the Netherlands) at the scan rate of 50 mV/s. The scan was reversed at the current of 10 μA. A glass cell designed for liquid-liquid interface experiments with an interfacial area of 0.159 cm^2 was a generous gift from professor Zdeněk Samec, J. Heyrovský Institute of Physical Chemistry, Prague. The cell is shown in Figure S1 and described in Scheme S1. Two reference electrodes (RE, Ag/AgCl), placed in Luggin capillaries to reduce *iR* drop, were used to measure the potential difference across the interface, while tungsten counter electrodes (CE) in both phases provided the electric current. The aqueous phase of organic reference (Ref. Water) had a cation (BA^+) in common with the supporting electrolyte of the organic phase to fix the potential across the respective interface. The potential was converted to the Galvani potential difference ($\Delta_o^w\phi$) by measuring the transfer potential of TEA^+ and correcting it to the reversible half-wave potential reported in the literature (0.116 V in DCB).[3]

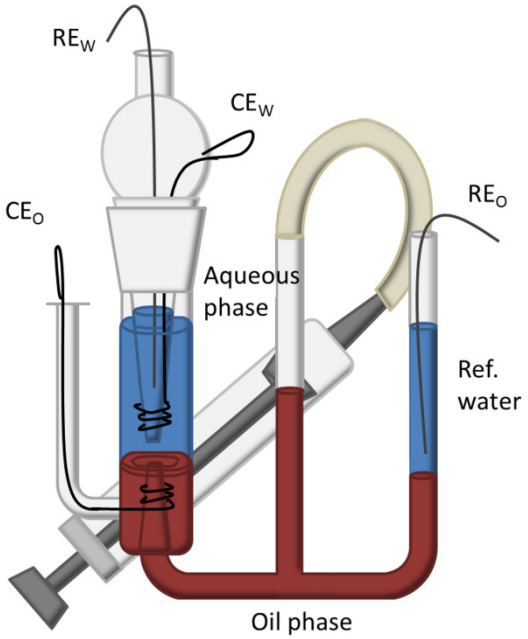

Figure S1. The four-electrode cell used for the cyclic voltammetry measurements.

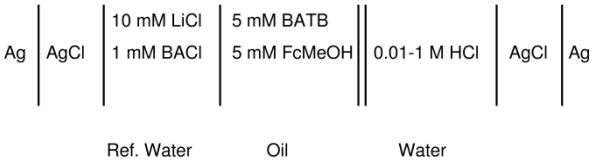

Scheme S1. The electrochemical cell used for the cyclic voltammetry measurements.

The voltammograms recorded at the oil-water interface of 5 mM BATB in DCB in the absence (baseline) and presence of 5 mM FcMeOH and in contact with different aqueous HCl solutions are shown in Figure S2. The positive end of the potential window is limited by proton transfer, and shifts in the negative direction with increasing proton concentration as dictated by the Nernst equation (data not shown). Adding FcMeOH to the organic phase shifts the positive end of the potential window by more than 100 mV in the negative direction, and the magnitude of the shift increases with increasing proton concentration. This indicates that FcMeOH facilitates proton transfer.

Furthermore, no return peak is observed after the reversal of the scan direction, indicating that the protons are consumed in the oil phase. This is similar to the proton coupled electron transfer wave observed for oxygen reduction by decamethylferrocene, where the latter acts as a proton acceptor to form a hydride species reacting with oxygen to form hydrogen peroxide.[4] However, DcMFc is a much stronger reducing agent (0.04 V vs. SHE),[5] and the proton transfer wave is shifted less with

DcMFc than with FcMeOH. If ferrocene (Fc), which has similar redox potential to FcMeOH, is used instead, the behaviour resembles the base line, indicating that the oxygen reduction by Fc is slow.[6] Very efficient catalysts like cofacial biscobalt porphyrins are needed to observe similar shift in the onset potential of proton transfer, and the sigmoidal shape of the wave.[2] The ferrocene derivatives without the –OH group are able to slightly facilitate proton transfer from water to oil phase by protonation of the metal core, and the rate of the following oxygen reduction reaction increases with decreasing redox potential (DcMFc > DMFc > Fc). Yet with FcMeOH the facilitation effect for H^+ transfer is very large and the rate of the following chemical reaction very high, comparable to reactions catalyzed by efficient oxygen reduction catalysts like cofacial biscobalt porphyrins.[2] This indicates that the reaction mechanism of FcMeOH and H^+ is very different from other ferrocene derivatives. The reaction mechanism can be described as facilitated proton transfer followed by chemical reaction.

The shift of ca. 70-90 mV with decreasing pH at the positive limit of the potential window indicates that the process is a one proton transfer per FcMeOH. The larger observed shift probably arises from differences in *iR* compensation between each measurement. When the experiment was done under the nitrogen atmosphere, the results were similar to those obtained in the presence of oxygen, confirming that molecular oxygen does not participate in the reaction.

Figure S2 also shows reversible chloride transfer at the negative limit of the potential window (wave potential shifts ca. 50-60 mV per log [Cl^-]), and an ion transfer wave at *ca.* 0.16 V assigned to $FcMeOH^+$. It is worth noticing that this wave is irreversible, indicating that $FcMeOH^+$ reacts further in the aqueous acidic solution.

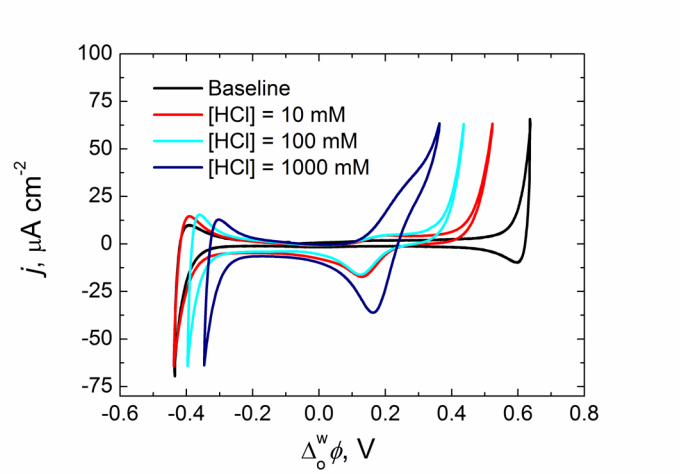

Figure S2. pH dependence of the voltammograms of 5 mM FcMeOH in DCB. Baseline: 5 mM BATB in DCB and 10 mM HCl.

The effect of the concentration of FcMeOH on the voltammogram at the oil-water (10 mM HCl) interface is shown in Figure S3: the baseline subtracted voltammograms are shown in the inset. The decrease in the concentration shifts the proton transfer wave to more positive potentials, and at 0.1 mM the voltammogram becomes almost identical with the base line. This shows that FcMeOH is able to facilitate proton transfer. At FcMeOH concentrations of 0.25 mM and 0.5 mM a diffusion limited peak for proton transfer is clearly visible, although it overlaps with the unassisted proton transfer wave. At 1 mM the transfer is independent of the FcMeOH concentration at the used conditions, as no peak is observed (a peak would be observed if the scan would be done at a slower scan rate to higher potentials). The base line subtracted voltammogram measured for 0.25 mM FcMeOH shows a clear irreversible peak with a half-wave potential of 0.57 V. The Nernst equation for this facilitated proton transfer process can be described as shown in eq. SI 1: [7]

$$\Delta_o^w\phi_{LH^+}^{1/2} = \Delta_o^w\phi_{H^+}^{o'} + \frac{RT}{2F}\ln\left(\frac{D_L}{D_{LH^+}}\right) - \frac{RT}{F}\ln K_{LH^+}c_{H^+,w} \qquad \text{(SI 1)}$$

where $\Delta_o^w\phi_{LH^+}^{1/2}$ and $\Delta_o^w\phi_{H^+}^{o'}$ are the observed half-wave potential and formal transfer potential of LH^+ and H^+ (0.677 V at the W/DCB interface), respectively. LH^+ stands for the protonated complex FcMeOH, D represents the diffusion coefficient of species in the oil phase, K_{LH^+} is the equilibrium constant of the protonation reaction of L and $c_{H^+,w}$ is the aqueous proton concentration. If the effect of the protonation on the diffusion coefficient of FcMeOH is assumed to be negligible, the association constant calculated from eq. (1) is 6450 M^{-1}. The calculated value is actually only the

apparent association constant, as the complexation may not reach equilibrium because of the following chemical reaction. However, the half-wave potential of the facilitated proton transfer does not shift significantly with increasing FcMeOH concentration, indicating that the effect of the chemical reaction step to the observed facilitated transfer is small.

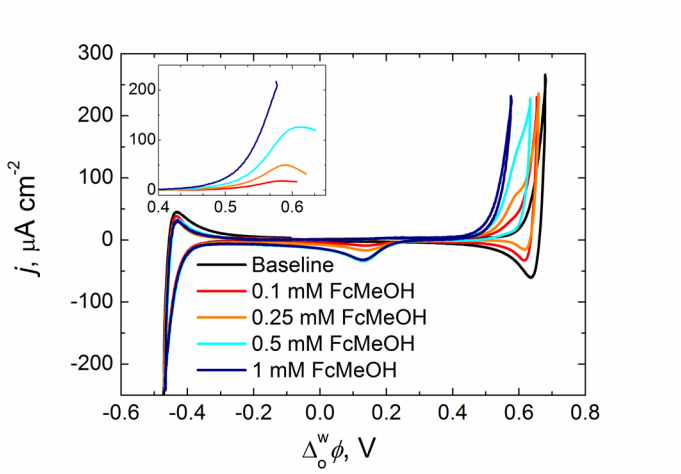

Figure S3. Effect of the FcMeOH concentration on the voltammetry, with the baseline subtracted positive scans shown in the inset (with 1 mM FcMeOH giving the highest current and 0.1 mM FcMeOH the lowest).

3.2 Ultramicroelectrode redox voltammetry

Ultramicroelectrode (UME) measurements were performed with 10 μm carbon fiber and 25 μm Pt electrodes, prepared as described earlier. [8] Briefly, a carbon fiber (Goodfellow, Oxford, UK) or a Pt wire (Goodfellow, Oxford, UK) was sealed in a glass capillary with a Bunsen flame and the seal was improved using a heating coil with vacuum in the capillary to avoid bubble formation. The electrical contacts to the microwires were made with soldering tin.

A Pt wire was used as the counter electrode. The reference electrode was a Ag/AgCl wire in a glass capillary filled with agarose gelled aqueous solution (1 mM BACl + 10 mM LiCl). The principle of the reference electrode is the same as for the reference electrode of the oil phase used in the four-electrode cell experiments. The potential scale was calibrated to the redox potential reported for DcMFc (0.67 V vs. Fc/Fc^{+}),[9] by adding trace amounts of DcMFc into the solution.

The voltammogram of 5 mM FcMeOH in DCB recorded at a 10 μm carbon UME is shown in Figure S4. In acetonitrile, FcMeOH has recently been shown to have two poorly resolved oxidation

peaks attributed to the dimerization of FcMeOH and $FcMeOH^+$.[10] If two distinct redox couples were present, these should be readily observed since TB^- is a weakly coordinating anion and DCB a solvent of a low donor number and relative permittivity.[11] However, only one redox reaction is observed here, hence no dimerization takes place in DCB under the conditions applied here. FcMeOH undergoes a reversible one electron redox reaction, like in aqueous solutions. The half-wave redox potential of FcMeOH was determined to be ca. -0.02 V vs. Fc/Fc^+ (or 0.72 V vs. aqueous SHE).

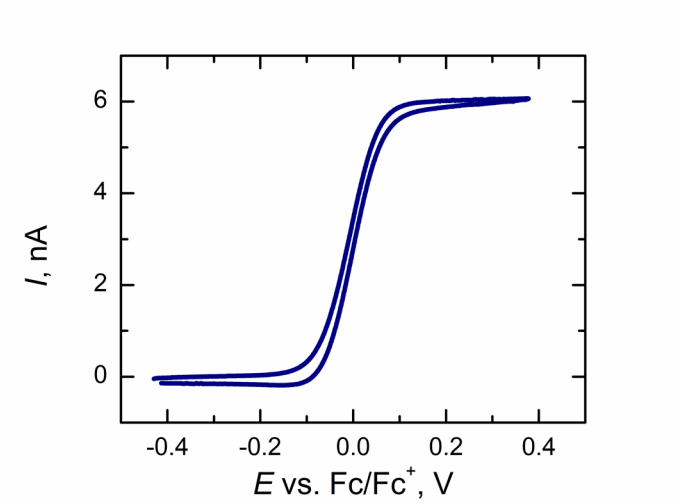

Figure S4. The CV of 5 mM FcMeOH + 5 mM BATB in DCB with 10 μm C UME, a scan rate of 20 mV s^{-1}.

The products of the shake flask reactions in the oil phase were also characterized by ultramicroelectrode measurements. After 10 minutes of reaction adsorption obviously blocked the surface of the carbon microelectrode, and no sigmoidal waves were observed. In contrast, on a Pt UME, a wave assigned for FcMeOH was observed (Figure S5), followed by a smaller wave on a positive scan. On the return scan a desorption peak followed by the FcMeOH redox wave was observed. This behaviour is probably due to the adsorption of the carbocation on the electrode surface. Also the response of the Pt UME is lost after longer reaction times, due to contamination of the surface as could be seen with an optical microscope.

However, if the reaction in the sample was quenched with equal amount of 5 mM DcMFc, clear sigmoidal waves could be observed, as shown in Figure S5. The addition of DcMFc has two effects on the system: i) DcMFc reduces most of the oxidized ferrocene derivatives, as it is strong reducing agent. ii) protons extracted in the oil phase are quickly consumed by oxygen and hydrogen peroxide reduction, catalyzed by the platinum wire, according to the following reactions:

$$2\mathrm{DcMFc} + \mathrm{O_2} + 2\mathrm{H^+} \xrightarrow{\text{cat.}} 2\mathrm{DcMFc^+} + \mathrm{H_2O_2} \quad \text{(SI 2)}$$

$$4\mathrm{DcMFc} + \mathrm{O_2} + 4\mathrm{H^+} \xrightarrow{\text{cat.}} 4\mathrm{DcMFc^+} + 2\mathrm{H_2O} \quad \text{(SI 3)}$$

$$2\mathrm{DcMFc} + \mathrm{H_2O_2} + 2\mathrm{H^+} \xrightarrow{\text{cat.}} 2\mathrm{DcMFc^+} + \mathrm{H_2O} \quad \text{(SI 4)}$$

$$2\mathrm{H_2O_2} \xrightarrow{\text{cat.}} \mathrm{O_2} + 2\mathrm{H_2O} \quad \text{(SI 5)}$$

Two clear oxidation waves in Figure S5 correspond well with the wave measured for pure FcMeOH and with the wave for FcCOOH at ca. 0.30 V vs. Fc/Fc^+, in agreement with the ESI-MS observations. The redox wave observed at –0.67 V corresponds to reduction/oxidation of DcMFc. The diffusion coefficients of 6.1×10^{-6} $cm^2\ s^{-1}$ for FcMeOH and 4.4×10^{-6} $cm^2\ s^{-1}$ for FcCOOH were determined from the limiting currents. Curiously, a sample taken after 20 min of reaction gave almost identical response as one taken after 30 min of reaction. After 45 min the signal had disappeared almost completely even for the quenched samples.

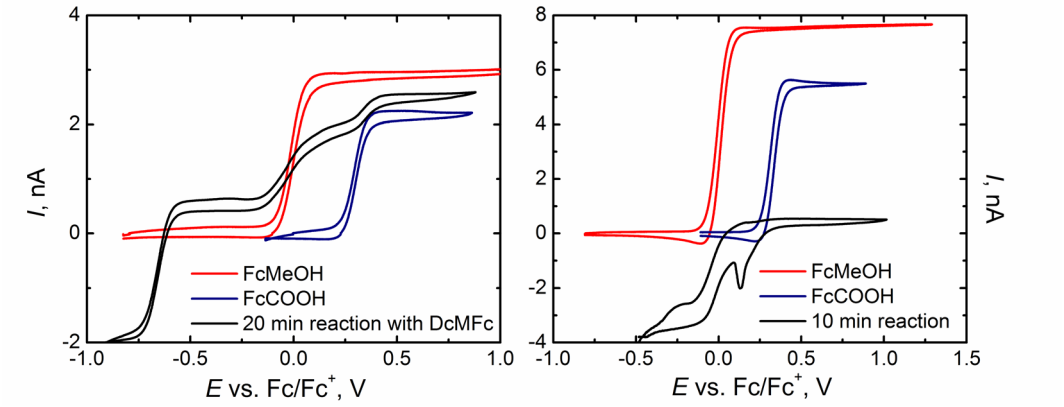

Figure S5. UME voltammograms of 2.5 mM FcMeOH and FcCOOH with 10 µm carbon fibre UME (Left) and with 25 µm Pt UME (Right). Left: voltammogram of the sample taken from the oil phase after 20 min reaction and quenched with DcMFc (10 µm carbon fibre UME). Right: UME voltammogram of the sample taken from the oil phase after 10 min reaction (25 µm Pt UME), not quenched.

The formation of the carbocation can be considered as an equilibrium reaction. Addition of DcMFc consumes protons and increases the amount of water in the system, driving the equilibrium towards FcMeOH. According to Figure 2 (main text), the formation of ester begins after 20 minutes of reaction, so the amount of observed FcCOOH and FcMeOH should decrease. However, this is not observed in UME measurements. Plausible explanations could be hydrolysis of the ester to FcCOOH and FcMeOH, or that the formation of ester does not have a significant effect on the redox potentials of the ferrocenyl groups.

4 Electrospray ionization mass spectrometry (ESI-MS) analysis

The relative abundance of the species as a function of time, analysed by ESI-MS, is shown in Figure S6.

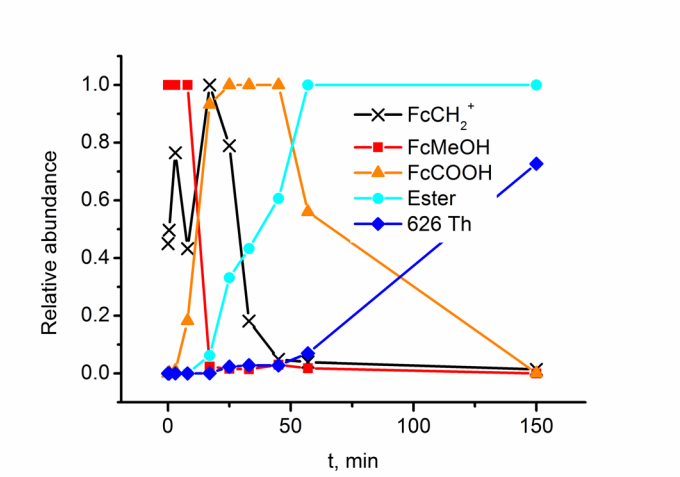

Figure S6. The relative abundance of the species as a function of time.

5 Partitioning of FcMeOH

Since FcMeOH is soluble in both aqueous and organic solvents, the partition coefficient between DCB and a hydrochloric acid solution was determined with the following procedure: 4 mL of DCB containing 5 mM FcMeOH and 5 mM BATB was equilibrated with 20 mL of 10 mM HCl for 3 hours or for 5 days in separate experiments, and the concentration of FcMeOH in the oil phase was determined at 448 nm by UV-Vis spectroscopy using a Varian Cary 50 instrument.

The partition coefficient of FcMeOH between DCB and water was calculated to be 82, based on the decrease of the absorption intensity of FcMeOH after 3 hours of equilibration time. A similar value was obtained after 5 day equilibration. Thus, FcMeOH does not significantly partition between the two phases.

6 Calculation of the Galvani potential difference across the liquid-liquid interface

In a system where ionic species of the two immiscible liquid phases are in equilibrium, the potential difference across the interface can be calculated with the Nernst-Donnan equation.[12]

$$\Delta_{\mathrm{o}}^{\mathrm{w}}\phi = \Delta_{\mathrm{o}}^{\mathrm{w}}\phi_{\mathrm{i}}^{0} + \frac{RT}{zF}\ln\frac{c_i^{\mathrm{o}}}{c_i^{\mathrm{w}}} \qquad \text{(SI 6)}$$

The mass balance for the species *i* is

$$n_{i,\,\mathrm{total}} = n_i^{\mathrm{o}} + n_i^{\mathrm{w}} \qquad \text{(SI 7)}$$

$$V_{\mathrm{o}}c_{i,\,\mathrm{initial}}^{\mathrm{o}} + V_{\mathrm{w}}c_{i,\mathrm{initial}}^{\mathrm{w}} = V_{\mathrm{o}}c_i^{\mathrm{o}} + V_{\mathrm{w}}c_i^{\mathrm{w}} \qquad \text{(SI 8)}$$

Additionally, electroneutrality condition of the both phases must be fulfilled:

$$\sum_i z_i c_i^{\mathrm{w}} = \sum_i z_i c_i^{\mathrm{o}} = 0 \qquad \text{(SI 9)}$$

In a case where $V_{\mathrm{o}} = V_{\mathrm{w}}$ combination of the equations (SI 6-9) gives

$$\sum_i z_i \frac{c_{i,\,\mathrm{total}}}{1+\exp\left[\frac{zF}{RT}(\Delta_{\mathrm{o}}^{\mathrm{w}}\phi - \Delta_{\mathrm{o}}^{\mathrm{w}}\phi_{\mathrm{i}}^{0})\right]} = 0 \qquad \text{(SI 10)}$$

Solution of the equation (SI 10) gives the Galvani potential difference of the system in equilibrium, and Nernst equation and mass balance equations can be used to calculate the equilibrium composition of both phases. The equilibrium concentrations between equal volumes of 5 mM LiTB + 10 mM HCl and neat 1,2-dichlorobenzene (DCB) are shown in Table S1. The standard transfer potentials of the species used in the calculations were estimated as described in the Supporting Information of ref. 9.

Table S1. Calculated equilibrium concentrations (mM) between neat DCB and 10 mM HCl and 5 mM LiTB in water.

	water	DCB
TB^-	2.81	2.19
H^+	7.89	2.11
Li^+	4.93	0.07
Cl^-	10.00	2.90×10^{-22}

References

[1] D. J. Fermín, H. D. Duong, Z. Ding, P. F. Brevet, H. H. Girault, *Phys. Chem. Chem. Phys.* **1999**, *1*, 1461-1467.

[2] P. Peljo, L. Murtomäki, T. Kallio, H.-J. Xu, M. Meyer, C. P. Gros, J.-M. Barbe, H. H. Girault, K. Laasonen, K. Kontturi, *J. Am. Chem. Soc.* **2012**, *134*, 5974-5984.

[3] B. Hundhammer, C. Müller, T. Solomon, H. Alemu, H. Hassen, *J. Electroanal. Chem.* **1991**, *319*, 125-135.

[4] B. Su, R. Partovi-Nia, F. Li, M. Hojeij, M. Prudent, C. Corminboeuf, Z. Samec, H. H. Girault, *Angew. Chem., Int. Ed.* **2008**, *47*, 4675-4678.

[5] J. J. Nieminen, I. Hatay, P. Ge, M. A. Méndez, L. Murtomäki, H. H. Girault, *Chem. Commun.* **2011**, *47*, 5548-5550.

[6] B. Su, I. Hatay, A. Trojánek, Z. Samec, T. Khoury, C. P. Gros, J. M. Barbe, A. Daina, P. A. Carrupt, H. H. Girault, *J. Am. Chem. Soc.* **2010**, *132*, 2655-2662.

[7] D. Homolka, L. Q. Hung, A. Hofmanova, M. W. Khalil, J. Koryta, V. Marecek, Z. Samec, S. K. Sen, P. Vanysek, *Anal. Chem.* **1980**, *52*, 1606-1610.

[8] H. Deng, P. Peljo, F. Cortés-Salazar, P. Ge, K. Kontturi, H. H. Girault, *J. Electroanal. Chem.* **2012**, *681*, 16-23.

[9] P. Peljo, T. Rauhala, L. Murtomäki, T. Kallio, K. Kontturi, *Int. J. Hydrogen Energy* **2011**, *36*, 10033-10043.

[10] W. L. Davis, R. F. Shago, E. H. G. Langner, J. C. Swarts, *Polyhedron* **2005**, *24*, 1611-1616.

[11] W. E. Geiger, F. Barrière, *Acc. Chem. Res.* **2010**, *43*, 1030-1039.

[12] T. Kakiuchi, in *Liquid-liquid interfaces, Theory and Methods* (Eds.: A. Volkov, G., D. W. Deamer), CRC Press, Boca Raton, **1996**, pp. 1-18.